Design and Experimentation of a Low-cost Receiver for Visible Light Communications

Wyatt Greives
Department of Electrical and Computer Engineering
California State University, Fresno
Fresno, CA 93740, U.S.A.
wgreives@mail.fresnostate.edu

Hovannes Kulhandjian*
Department of Electrical and Computer Engineering
California State University, Fresno
Fresno, CA 93740, U.S.A.
hkulhandjian@mail.fresnostate.edu

***Abstract*—Visible light communication (VLC), an emerging field of research, requires the use of visible light, optical sensors, transimpedance amplifiers (TIA), and filtration circuitry. As processing is done with voltages, TIAs convert the current from the optical source into a voltage. In this paper, we propose a low-cost receiver for long-range visible light communications. The receiver is composed of a wide bandwidth TIA using an off the shelf operational amplifier (op-amp). The design process focuses on the calculations for feedback resistance and capacitance, and other op-amp stabilization techniques for the receiver. We test the proposed receiver along with the TIA using the National Instruments simulator tool Multisim to determine the optimum operational bandwidth. The proposed VLC system is developed and experimented on a testbed composed of the transmitter circuitry, designed receiver, and National Instrument's USB-6351 data acquisition board for analog-to-digital (ADC) and digital-to-analog (DAC) conversion operations. Random data bit stream at a bit rate of $50\ kb/s$ is transmitted using on-off keying (OOK) modulation scheme. We study the bit-error rate (BER) performance for different transmitter and receiver distances up to $860\,cm$. The experimental results reveal that for a distance of $380\,cm$ a BER of 9.76×10^{-5} is achieved.**

***Index Terms*—Visible light communication (VLC), transimpedance amplifier (TIA), VLC receiver design.**

I. Introduction

Visible light communication (VLC) has attracted a lot of attention by the research community in recent years. VLC can be used in 5G communication with applications in the medical field, airplane high-data rate communication, and indoor localization, to name a few. VLC systems utilize visible light to transmit data through free-space, which is considered a subset of free-space optical communication. In a VLC system, the transmitter utilizes light-emitting diodes (LEDs) to serve the dual purpose of illumination and communication—LEDs are less expensive, have faster switching speeds and are more energy/heat efficient compared to traditional lighting (incandescent and fluorescent). The receiver is composed of optical sensors (image sensors or photodiodes), amplification, and filtration circuitry. VLC systems can deliver a large, unregulated bandwidth with the capabilities to expand upon current communications infrastructures by providing secure indoor networks and positioning [1], [2]; underwater communications [3], [4], [5]; and intelligent transportation systems [6], [7], [8].

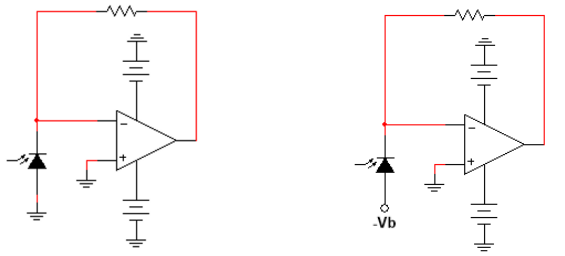

(a) Photovoltaic mode. (b) Photoconductive mode.

Fig. 1: Op-amp TIA configurations.

Optical receivers composed of photodiodes require transimpedance amplification circuitry to convert the low photodiode currents into a proportional voltage signal. In Fig. 1, two typical op-amp based TIA configurations are shown. Figure 1a shows a TIA operating in photovoltaic mode with the anode of the photodiode connected to ground; this topology exhibits low-noise characteristics and works well in low-light applications with frequencies up to $350\ kHz$ [9]. Figure 1b shows a TIA operating in photoconductive mode with the anode of the photodiode connected to a reverse bias voltage; this mode of operation can increase the response speed by decreasing the junction capacitance of the photodiode, but will introduce more noise in the form of dark current [9]. The transimpedance gain of the TIA circuit that is set by the feedback resistor and a feedback capacitor is often included in the design process to account for the frequency response of the photodiode and op-amp components. In order to design and implement an efficient VLC optical receiver, one needs to carefully select the photodiode(s) and op-amp devices, and fine-tune the design parameters for the optimum performance.

In [10] a high performance op-amp is used to design a moderate bandwidth, low-noise TIA for detecting smaller magnitude signals in LIDAR applications. High data rate transmission for short distances ($20\,cm - 100\,cm$) was achieved in [11] using a remaining carrier sweeping out LED driver and a BPW34 photodiode. An OPA656 op-amp was used in [12] to design an analog front-end (AFE) with a wide $1\ MHz$ bandwidth and moderate gain for a short-range ($50\ cm$) VLC system. Noise analysis was performed on the

*Corresponding author.
This work was partially supported by Fresno State Transportation Institute (FSTI) and DPS Telecom grants.

978-1-7281-8903-1/20/$31.00 ©2020 IEEE

OPA656 in [13] with results indicating a lower feedback resistor is recommended for low-noise TIA characteristics. In-depth TIA design, simulation, and experimentation using transistors instead of op-amps was performed in [14], [15], and [16], exhibiting low-noise characteristics, large bandwidths, and high data rates (Gb/s). A low-noise, high-gain TIA design was developed in [17] for measuring short signal pulses in photometer readings. A high-speed, real-time VLC system was designed using discrete components for the TIA in [18] utilizing pre-emphasis and post-equalization circuits to achieve a $550\,Mb/s$ data rate at a distance of $60\,cm$.

Unlike previous research work which mainly focused on studying the effects of noise in the visible light communication channel, and are mostly tested for short range communications, instead; our main focus is to design a low-cost photovoltaic TIA circuitry along with a VLC system composed of a transmitter and receiver that can provide low BER for fairly large distances. The proposed VLC system is developed and experimented on a testbed composed of the transmitter circuitry, designed receiver, and National Instrument's USB-6351 data acquisition board for analog-to-digital (ADC) and digital-to-analog (DAC) conversion operations. Random data bitstream at a bit rate of $50\ kb/s$ is transmitted using on-off keying (OOK) modulation scheme. We study the bit-error-rate (BER) performance for different transmitter and receiver distances up to $860\,cm$. The experimental results reveal that for a distance of $380\,cm$, a BER of 9.76×10^{-5} was achieved.

The rest of the paper is organized as follows. In Section II, we present the proposed VLC system, design process for an op-amp based TIA, and transmitter design. In Section III, we present the simulation results of the proposed TIA along with the optimum parameter selection. In Section IV, we present the experimental setup, methods and results of the proposed VLC system. Finally, in Section V, we draw the main conclusions and present future works.

II. System Description

In this section, we discuss the VLC system model as well as the VLC receiver design.

A. Overall VLC System

Figure 2 shows the block diagram of the VLC system. The generated data bits are first encoded using a modulation scheme. The encoded data is converted to an analog signal using a DAC to interface with an LED driver circuit. The circuit drives the LED outputting the encoded data by modulating the light intensity. The line-of-sight (LOS) component of the light signal is collected by the receiver's photodiode(s) along with external light interference and is converted to a current. The current is then converted into a proportional voltage using the TIA, adding electrical noise interference in the process. The voltage is filtered, amplified, and sampled, by the low-pass filter (LPF), amplifier and ADC components, where it can be decoded at the receiver side. The main points of emphasis in electrical design for a VLC system revolve around the receiver and transmitter.

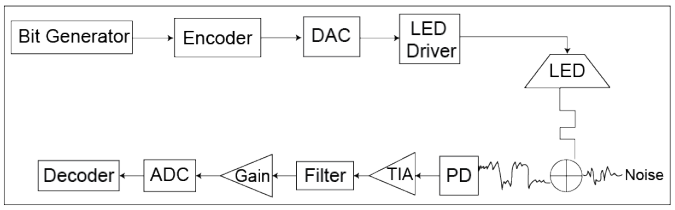

Fig. 2: VLC system diagram.

Our proposed receiver is composed of two BPW34 photodiodes, an OPA656 op-amp, and a low-pass filter to reduce noise interference. The design process focuses on optimizing the TIA for large bandwidth and low-voltage signal processing. By modeling the OPA656 op-amp's transfer function and the feedback network produced by the TIA-photodiode combo, an optimal feedback capacitance can be calculated and simulated.

The transmitter's LED driver circuit is composed of two TIP31C transistors and a Chanzon $3\ W$ LED. The circuit design focuses on producing high current through the LED from a low current DAC source, in accordance with OOK modulation.

B. Receiver Design

The maximum output voltage of the TIA is determined by its feedback resistor and the maximum generated current of the photodiode. The maximum current of the BPW34 photodiode is determined from its relative spectral sensitivity, shown in Figure 3.

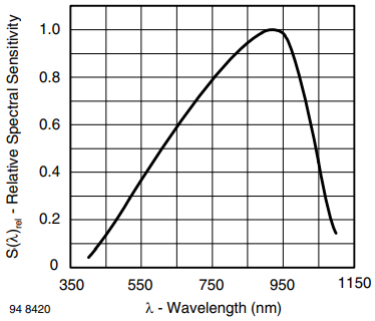

Fig. 3: Relative spectral sensitivity of BPW34 photodiode [19].

Due to white light being composed of all wavelengths of visible light, the peak spectral sensitivity for the BPW34 photodiode is averaged to about 0.6. The typical current for the BPW34 is about $50\,\mu A$ [19], yielding about $30\,\mu A$ for one photodiode. Experimentally, the maximum photodiode current for the BPW34 is determined to be about $20\ \mu A$. As there were two photodiodes in the design, the maximum expected current is about $40\ \mu A$. Calculation of the feedback resistor used in the TIA design is determined by:

$$R_f = \frac{V_{out,max} - V_{out,min}}{I_{PD,max}} = \frac{1V - 0V}{40\mu A} = 25\,k\Omega. \quad (1)$$

The junction capacitance of the photodiode is important in determining the frequency response of the circuit. The junction capacitance of the BPW34 operating in photovoltaic mode is about $72\,pF$. Since there were two photodiodes used in the design, this yields a total diode capacitance of $144\,pF$. The differential and common-mode capacitance of the OPA656

are $0.7\ pF$ and $2.8\ pF$, respectively [20]. Since the diode capacitance and op-amp input capacitance are in parallel the total input capacitance is determined by:

$$C_{in} = C_J + C_{diff} + C_{CM} = 147.5\,pF. \tag{2}$$

The parasitic input capacitance of the photodiode and op-amp create an undesired pole in the TIA loop transfer function. The feedback resistance and input capacitance of the circuit create a feedback network that can be modeled with the following transfer function [21], using the results of (1) and (2):

$$\beta(s) = \frac{1}{1 + sR_fC_{in}} = \frac{1}{1 + s(3.69 \times 10^{-6})}. \tag{3}$$

Additionally, the DC open-loop gain (A_{OL}) of the op-amp has an associated transfer function. The DC open-loop gain for the OPA656 is rated at $65\,dB$ [20]. The gain-bandwidth product (GBWP) of the OPA656 is rated at $230\ MHz$. To account for variation in the process corners of the gain-bandwidth product frequency, 60% of the rated $230\ MHz$ is used for the calculations [21]. To find the $-3\,dB$ corner frequency for the op-amp's DC open-loop transfer function, we calculate it as:

$$\omega_o = \frac{\text{GBWP}}{10^{\frac{A_{OL}-3}{20}}} = \frac{0.6(230 \times 10^6)}{10^{\frac{62}{20}}} = 109,617\,rad/s. \tag{4}$$

Using the result from (4), the open-loop gain frequency transfer function of the OPA656 is modeled as:

$$A(s) = A_{OL} \times \frac{\omega_o}{s + \omega_o} = \frac{195 \times 10^6}{s + 109,617}. \tag{5}$$

The reciprocal of the feedback network in (3) and the open-loop gain frequency in (5) are plotted in MATLAB to determine the rate of closure for the system, shown below in Figure 4a.

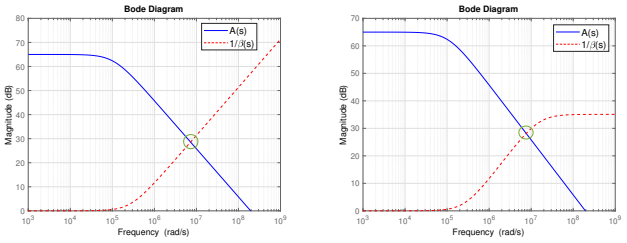

(a) Without feedback capacitor. (b) With feedback capacitor.

Fig. 4: Rate of closure for TIA system.

The rate of closure (ROC) of the system at the crossover frequency is defined as the difference between the slopes of $\frac{1}{\beta(s)}$ and $A(s)$, determined to be $+20dB/dec$ and $-20dB/dec$ from Figure 4a, respectively. The ROC for the TIA without a feedback capacitor is determined by:

$$ROC = \left|\frac{1}{\beta(s)}\right|_{Slope} - \left|A(s)\right|_{Slope} = 40\,dB/dec. \tag{6}$$

The phase margin (ϕ_m) of the system at the crossover frequency is approximated using the following equation and the calculated ROC from (6):

$$\phi_m \cong 180^\circ - 4.5 \times ROC = 0^\circ. \tag{7}$$

Improving the phase margin of the circuit effectively improves reception of the incoming signal. Since the modulation scheme is OOK, it is necessary to have a large TIA bandwidth in order to not degrade the harmonics of the transmitted square pulses. By adding a feedback capacitor to the TIA, a zero can be introduced into the feedback network transfer function. In doing so, the slope of $\frac{1}{\beta(s)}$ at the intersection with $A(s)$ decreases, which leads to a smaller ROC and an increased phase margin at the crossover frequency. To achieve a phase margin of 45° the feedback capacitor is designed for optimal compensation. The intercept frequency is defined as:

$$f_{int} = \frac{1}{2\pi \times R_f \times C_f}. \tag{8}$$

The intercept frequency (f_{int}) for optimal compensation falls halfway between the corner frequency of the feedback network (f_{fb}) and the $0\,dB$ crossover frequency for the GBWP of the op-amp. Since the scales are logarithmic this leads to f_{int} being the geometric mean of f_{fb} and the GBWP of the op-amp, hence,

$$f_{int} = \sqrt{f_{fb} \times \text{GBWP}}, \tag{9}$$

$$f_{fb} = \frac{1}{2\pi \times R_f(C_f + C_{in})}. \tag{10}$$

Substituting (8) and (10) into (9) yields:

$$\frac{1}{2\pi \times R_fC_f} = \sqrt{\frac{\text{GBWP}}{2\pi \times R_f(C_f + C_{in})}}. \tag{11}$$

Through algebraic manipulation a quadratic polynomial is established with the positive root representing the feedback capacitance for optimal compensation of the TIA. Substituting the values from (1) and (2) the feedback capacitor is calculated as:

$$C_f = \frac{1 + \sqrt{1 + (8\pi \times R_f \times C_{in} \times \text{GBWP})}}{4\pi \times R_f \times \text{GBWP}} = 2.63\,pF. \tag{12}$$

The feedback network for the circuit is modeled by the following transfer function:

$$\beta(s) = \frac{1 + sR_fC_f}{1 + sR_f(C_f + C_{in})} = \frac{1 + s(6.6 \times 10^{-8})}{1 + s(3.75 \times 10^{-6})}. \tag{13}$$

The reciprocal of the feedback network in (13) and the open-loop gain transfer function of the op-amp in (5) are plotted in MATLAB to determine the rate of closure for the designed TIA system, shown in Figure 4b.

The ROC of the TIA-photodiode system with a feedback capacitor decreases due to the drop in the slope of β at the crossover frequency. ϕ_m is determined to be approximately 30°, within range for a stable system.

The TIA circuit is shown in Figure 5a. The rails of the op-amp are connected to $\pm 5\ V$, with decoupling capacitors connected between each supply pin and ground. Due to the photodiode being an AC-coupled source, a DC return path is introduced at the inverting input with a $1\ M\Omega$ resistor—this prevents the voltage output of the amplifier from saturating to one of the op-amp's rails over time [22].

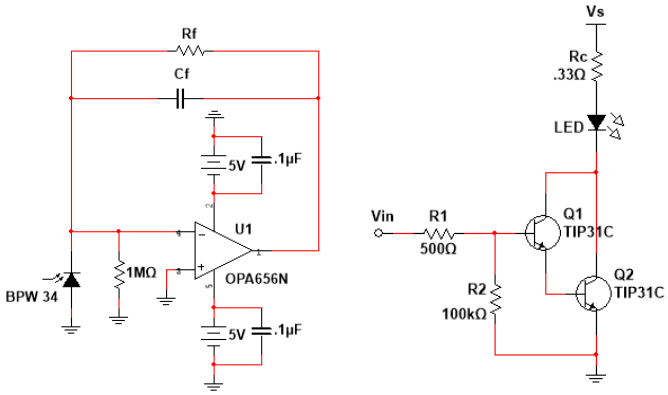

(a) TIA circuit design. (b) Tx LED driver circuit.

Fig. 5: Multisim circuit design.

C. Transmitter Design

Figure 5b shows the LED driver circuit design for the transmitter (Tx). Two TIP31C bipolar junction transistors (BJTs) are used in a Darlington pair configuration to provide a larger current amplification from the low-current input. The TIP31C BJTs also serve as extra power dissipation to prevent overloading the LED. The Darlington pair drives the Chanzon $3\,W$ LED, with a small series resistance of $0.33\,\Omega$, to limit the current through the LED. Resistors R1 and R2 bias the transistors and R2 is a current return path during the LED's turn-off time. The input controlling the base of the transistor is connected to the NI USB-6351 DAC output. The supply voltage (Vs) was adjusted to achieve two different light intensities—low light intensity, with a current of $75mA$, and low-medium light intensity, with a current of $145mA$.

III. Simulation

In this section, we present the simulation results for the proposed TIA design.

A. Simulation Model

The circuit is simulated in Multisim, as shown in Figure 6 below. The model for the BPW34 photodiode array is a current source and a parallel capacitor that represents the equivalent junction capacitance.

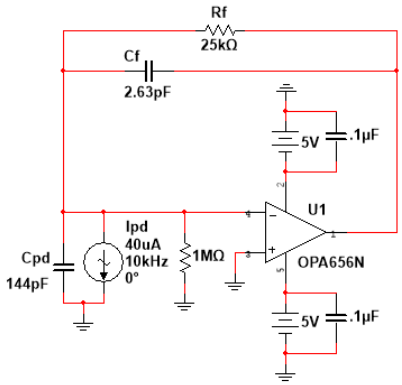

Fig. 6: TIA Multisim model.

An AC sweep is performed from $10\,Hz$ to $1\,GHz$ on the input current and output voltage of the TIA, and a Bode plot of the magnitude and phase is generated.

B. Simulation Results

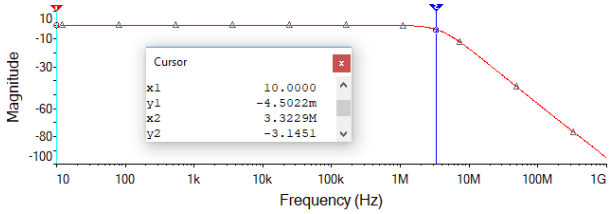

(a) Magnitude plot.

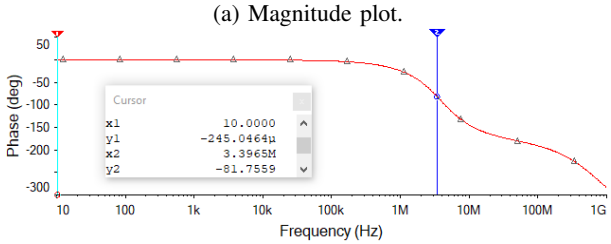

(b) Phase plot.

Fig. 7: TIA Bode plot.

Figure 7a shows the results of the magnitude Bode plot performed on the simulation model. The $-3\,dB$ cutoff frequency is measured to be about $3.3\,MHz$, and the max voltage is about $1\,V$, as calculated in the design section.

Figure 7b shows the results of the phase Bode plot performed on the simulation model. At the cutoff frequency the phase is determined to be about $-89°$, providing a stable bandwidth.

IV. Experimentation

In this section, we present the testbed experimental results for the proposed VLC system.

A. Experimental Setup

The VLC experimentation is carried out on the developed testbed, shown in Fig. 8.

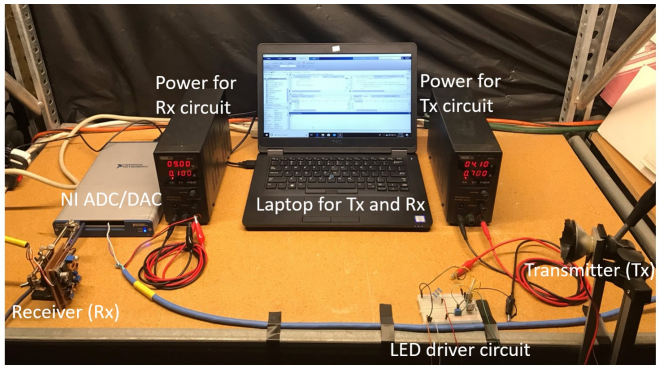

Fig. 8: Testbed experimentation.

The receiver circuit is implemented on perfboard, as shown in Figure 9. A XL4005 Buck converter is used to step down

$9\,V$ to $5\,V$. A charge-pump circuit using a 555 timer chip is used to convert $9\,V$ into $-5\,V$. The $\pm 5\,V$ is clamped using zener diodes and delivers power to the OPA656 op-amp.

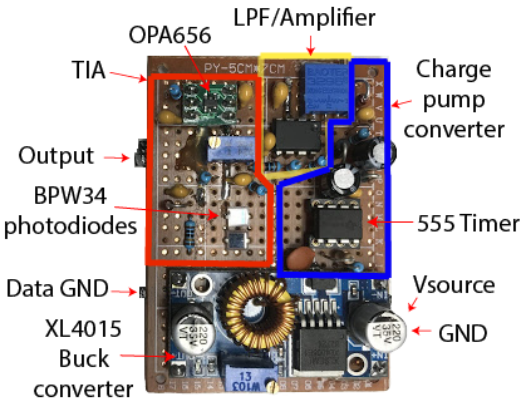

Fig. 9: Receiver circuit implementation on perfboard.

The transmitter circuit is implemented on a breadboard and is shown in Figure 10. The LED, attached to a tripod, is surrounded by a shroud to focus the light, as shown in Figure 11.

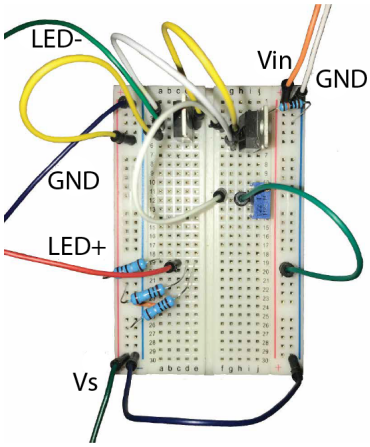

Fig. 10: LED driver circuit on breadboard.

Fig. 11: LED transmitter on a tripod.

Figure 12 shows the experimental block diagram for the designed VLC system. The optical channel voltage is measured and recorded with the transmitter LED "OFF" and with the LED "ON". A random stream of 1 million bits is generated in MATLAB and appended to a 100-bit preamble used for synchronization purposes at the receiver side. The encoded bits are sent to the NI USB-6351 DAC board to output a voltage signal $(0 - 4\,V)$ at a rate of $50\,kHz$ that toggles the LED

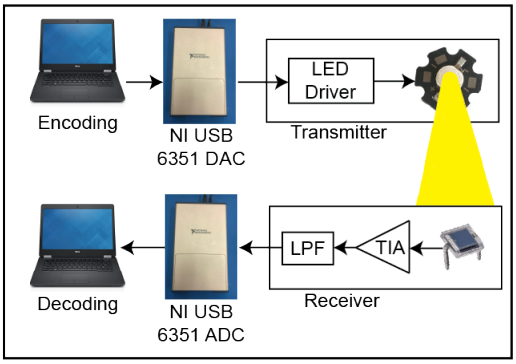

Fig. 12: VLC system block diagram.

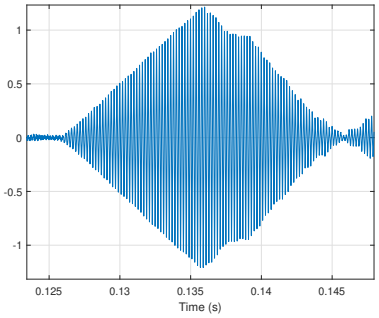

Fig. 13: Preamble detection using matched filter.

"OFF" and "ON", respectively. This modulated OOK light signal propagates through the wireless optical channel where it is collected by the receiver. The large bandwidth $(3.3\,MHz)$ of the receiver increases the fidelity of the digital pulses in reception. The output voltage from the receiver is sampled by the NI USB-6351 ADC at a rate of $500\,kSamples/s$ and put through a matched filter using the known preamble to find the start of the transmitted data. Figure 13 shows the peak that results from autocorrelating the 100-bit preamble with the received data. From the start of the received data stream, the voltage samples are averaged and demodulated using a hard decision threshold set between the average noise level and light level. The experiments are performed on two different average light levels (low and low-medium light intensity) for the transmitter LED. The BER is calculated by comparing the received data and the transmitted data.

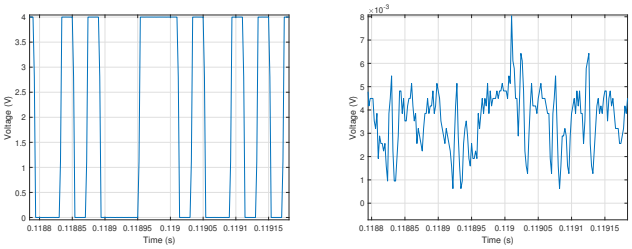

(a) Transmitted signal. (b) Received signal.

Fig. 14: Transmitted signal and received signal.

B. Experimental Results

Figure 14a shows the transmitted binary signal voltage and Figure 14b shows the sampled voltage signal at the output of the receiver for a distance of 4 meters at low-medium light intensity. The received signal's voltage is in the range of $0 - 10\,mV$ throughout the various trials, as shown in Fig. 14b.

Figure 15 shows the BER performance as a function of distance for a low light intensity. The range for the distance is between $120\,cm$ and $300\,cm$, with a BER less than 10^{-6} being recorded for distances less than $100\,cm$. We can see that at about $120\,cm$ the BER is 2×10^{-4}.

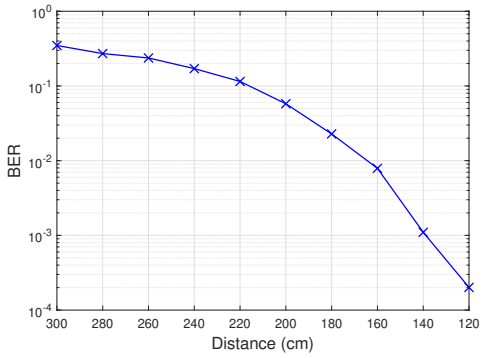

Fig. 15: BER vs distance for low light intensity.

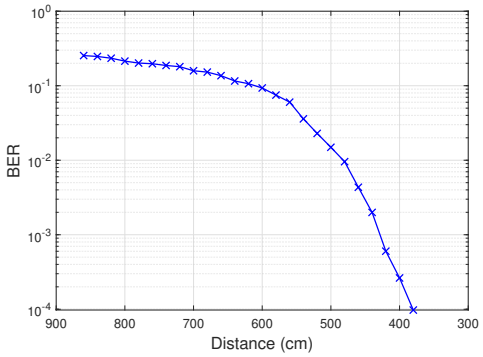

Fig. 16: BER vs distance for low-medium light intensity.

Figure 16 shows the BER performance as a function of distance for a low-medium light intensity. The range for the distance is between $380\,cm$ and $860\,cm$, with a BER less than 10^{-6} being recorded for distances less than $380\,cm$. We can see that at about $380\,cm$ the BER is 9.76×10^{-5}.

V. Conclusion

In this paper, we presented the design and experimentation of a low-cost, large bandwidth TIA for receiving optical transmissions in a VLC system utilizing BPW34 photodiodes and an OPA656 op-amp. Testbed experimentation was carried using the proposed VLC system transmitter and receiver circuitry using on-off keying (OOK) modulation. Experiments showed the correlation between transmitter-receiver distance and BER for two distinct light intensities; a BER of 9.76×10^{-5} was achieved for $50\,kb/s$ transmission over $380\,cm$ range.

Future works will focus on using different modulation schemes, improving transmitter design, increasing transmitter-receiver distance, non-LOS effects on transmission, increasing data rates, and outdoor applications of VLC.

References

[1] H. Chun, A. Gomez, C. Quintana, W. Zhang, G. Faulkner, and D. O'Brien, "A wide-area coverage 35 Gb/s visible light communications link for indoor wireless applications," *Scientific reports*, vol. 9, no. 1, pp. 1–8, 2019.

[2] L. A. Azizan, M. S. Ab-Rahman, M. R. Hassan, A. A. A. Bakar, and R. Nordin, "Optimization of signal-to-noise ratio for wireless light-emitting diode communication in modern lighting layouts," *Optical Engineering*, vol. 53, no. 4, p. 045103, April 2014.

[3] S. Hessien, S. C. Tokgöz, N. Anous, A. Boyacı, M. Abdallah, and K. A. Qaraqe, "Experimental evaluation of ofdm-based underwater visible light communication system," *IEEE Photonics Journal*, vol. 10, no. 5, pp. 1–13, Sept. 2018.

[4] F. Wang, Y. Liu, F. Jiang, and N. Chi, "High speed underwater visible light communication system based on LED employing maximum ratio combination with multi-PIN reception," *Optics Communications*, vol. 425, pp. 106–112, 2018.

[5] M. V. Jamali, P. Nabavi, and J. A. Salehi, "MIMO underwater visible light communications: Comprehensive channel study, performance analysis, and multiple-symbol detection," *IEEE Transactions on Vehicular Technology*, vol. 67, no. 9, pp. 8223–8237, 2018.

[6] R. M. Marè, C. E. Cugnasca, C. L. Marte, and G. Gentile, "Intelligent transport systems and visible light communication applications: An overview," in *Proc. of IEEE International Conf. on Intelligent Transportation Systems (ITSC)*, Rio de Janeiro, Brazil, 2016, pp. 2101–2106.

[7] N. Kumar, "Visible light communication based traffic information broadcasting systems," *International Journal of Future Computer and Communication*, vol. 3, no. 1, p. 26, 2014.

[8] H. Kulhandjian, "A Visible Light Communications Framework for Intelligent Transportation Systems," Mineta Transportation Institute Publications, Tech. Rep., Project No. 1911, August 2020.

[9] O. OptoElectronics, "Photodiode Characteristics and Applications."

[10] A. Auckloo, R. Tozer, J. David, and C. H. Tan, "A low noise op-amp transimpedance amplifier for LIDAR applications," in *Proc. of IEEE International Conference on Electronics, Circuits and Systems (ICECS)*, Marseille, France, Dec. 2014, pp. 590–593.

[11] T. K. Khani, H. B. Mangrio, and F. A. Umrani, "Performance Analysis of VLC system using Commercially Available Components," in *Proc. of IEEE International Multitopic Conf. (INMIC)*, Nov. 2019, pp. 1–4.

[12] S. Fuada, A. P. Putra, Y. Aska, and T. Adiono, "Trans-impedance amplifier (HA) design for Visible Light Communication (VLC) using commercially available OP-AMP," in *Proc. of International Conference on Information Technology, Computer, and Electrical Engineering (ICITACEE)*, Semarang, Indonesia, Oct. 2016, pp. 31–36.

[13] T. Adiono, R. V. W. Putra, and S. Fuada, "Noise and Bandwidth Consideration in Designing Op-Amp Based Transimpedance Amplifier for VLC," *Bulletin of Electrical Engineering and Informatics*, vol. 7, no. 2, pp. 314–322, June 2018.

[14] J. P. L. A. D. M. Carvalho, "Design of a transimpedance amplifier for an optical receiver," Ph.D. dissertation, 2017.

[15] B. Abdollahi, P. Akbari, B. Mesgari, and S. Saeedi, "A low voltage low noise transimpedance amplifier for high-data-rate optical recievers," in *Proc. of IEEE Iranian Conf. on Elect. Eng.*, May 2015, pp. 1187–1192.

[16] R. Y. Chen and Z. Yang, "CMOS Transimpedance Amplifiers for Optical Wireless Communications," in *Proc. of IEEE International Symposium on Intelligent Signal Processing and Communication Systems*, Okinawa, Japan, Nov. 2013, pp. 505–508.

[17] P. Patil, G. Mukherjee, A. Sharma, and R. Mudholkar, "High-gain transimpedance amplifier (TIA) for night airglow photometer," *International Journal of Electronic Eng. Research*, vol. 1, no. 2, pp. 109–116, 2009.

[18] H. Li, X. Chen, J. Guo, and H. Chen, "A 550 Mbit/s real-time visible light communication system based on phosphorescent white light LED for practical high-speed low-complexity application," *Optics express*, vol. 22, no. 22, pp. 27 203–27 213, 2014.

[19] *Silicon PIN Photodiode, BPW34, BPW34S*, Vishay Semiconductors, Aug. 2011, Rev. 2.1. [Online]. Available: http://www.vishay.com/docs/81521/bpw34.pdf

[20] *OPA656 Wideband, Unity-Gain Stable, FET-Input Operational Amplifier*, Texas Instruments, 2011, Rev. Sept. 2015. [Online]. Available: http://www.ti.com/lit/ds/symlink/opa656.pdf

[21] A. Bhat, "Stabilize your transimpedance amplifier," 2012.

[22] C. Kitchin, "Avoid Common Problems When Designing Amplifier Circuits," *Analog Dialogue*, vol. 41, no. 3, pp. 1–7, Aug. 2007.